Geocarto International

ISSN: (Print) (Online) Journal homepage: https://www.tandfonline.com/loi/tgei20

A hyperspectral R based Leaf Area Index estimator: Model development and implementation using AVIRIS-NG

Prachi Singh, Prashant K. Srivastava, R. K. Mall, Bimal K Bhattacharya & Rajendra Prasad

To cite this article: Prachi Singh, Prashant K. Srivastava, R. K. Mall, Bimal K Bhattacharya & Rajendra Prasad (2022): A hyperspectral R based Leaf Area Index estimator: Model development and implementation using AVIRIS-NG, Geocarto International, DOI: 10.1080/10106049.2022.2071476

To link to this article: https://doi.org/10.1080/10106049.2022.2071476

A hyperspectral R based Leaf Area Index estimator: Model development and implementation using AVIRIS-NG

Prachi Singh[1,2], Prashant K. Srivastava[1,2,*], R. K. Mall[2,*], Bimal K Bhattacharya[3], Rajendra Prasad[4]

[1]Remote Sensing Laboratory, Institute of Environment and Sustainable Development, Banaras Hindu University, U.P. 221005

[2]DST-Mahamana Centre for Excellence in Climate Change Research, Institute of Environment and Sustainable Development, Banaras Hindu University, Varanasi, 221005 India

[3]Space Applications Centre (ISRO) Ahmedabad, Gujarat, India

[4]Indian Institute of Technology BHU Varanasi, Department of Physics, Varanasi, 221005 India

[*]Corresponding author: prashant.just@gmail.com; rkmall@bhu.ac.in

Abstract

Hyperspectral Remote Sensing (HRS) data is vital for crop growth monitoring due to availability of contiguous bands. This research work provides a new novel crop estimator model given the name "Crop Stage estimator" developed using the HRS on an open-source R platform. The generic model structure provides an easy way to test and modify the importance of crop parameters namely Leaf Area Index to deduce crop growth stages of winter wheat (*Triticum aestivum* L.) at different crops growth stages –heading, tillering and booting. Further, to know the LAI variations on different agriculture sites, the best model was implemented using the AVIRIS-NG (Airborne Visible Near-Infrared Imaging Spectrometer - Next Generation) hyperspectral datasets for LAI estimation. The analysis indicates that during tillering stage the performance was found best during calibration (r =0.66, RMSE =0.40, and Bias =-0.80) and validation (r =0.98, RMSE =0.20, and Bias =0.12) in comparison to the ground measurements.

Keywords: Crop Stage; LAI, Simulation; Spectroradiometer, Hyperspectral, AVIRIS-NG.

1. Introduction

The rapid rise in human populations along with factors like climate change and declining natural resources have created pressure on the agricultural sector to ensure food security. In this context, crop modelling proves to be a powerful tool having a great potential for expanding crop yield (Mbow et al. 2017; Shukla et al. 2019). Crop simulation models are the representation of simplified crop production systems consisting of nonlinear mathematical equations and logic to provide a systematic analysis of the crop production system (Bouman et al. 1996; Malhi et al. 2020). They are continuous dynamic systems that precisely explain yield in terms of various growth processes and the effect of environmental factors on each growth process (Aggarwal 2002; Park et al. 2005). The models may be simple and describe a single process or they may be composed of more mathematical equations which describe the different processes such as photosynthesis, phenology, carbon assimilation and partitioning, soil water availability, plant growth and development and response to water or nutrient deficiency (Bowen et al. 2002; Anand et al. 2021). Hence, the model integrates the effect of different factors on productivity and provides a unique opportunity to supplement and extrapolate the results of field trials (Aggarwal 2002; Srivastava et al. 2021). Thus, it's application extends getting information of potential yield, nutrient and water requirement of the crop, management practices for

biotic and abiotic stresses, impact due to climate change and and selection of crops and varieties for optimum production (Wolday and Hruy 2015; Silva et al. 2021).

Leaf Area Index or LAI is expressed as the leaf area per unit of the ground surface area in broadleaf canopies and for the coniferous canopies is one-half the total needle surface area per unit ground area of a plant. It is considered a cardinal indicator of the plant growth rate and hence aids in determining various stages of the crop. It also helps in estimating crop water stress and the health of the crop (Fang et al. 2019; Yu 2020). To understand the geometry of vegetation canopy and ecological processes at global and regional scale leaf area index proved to be an important parameter. LAI also plays an important role in the conduction of photosynthesis processes of vegetation (Chapin et al. 2006). Crop growth dynamics and seasonal evolution of vegetation can be depicted using the LAI information. LAI estimation can be done using both destructive and non-destructive techniques. Lab-based LAI estimation though is precise, yet are not applicable for extensive and large area related studies (Tao et al. 2020). Non-destructive measurement using advanced remote sensing data is a more cost-effective, reliable and time-saving and comparative assessment with other methods makes it more suitable for large-scale and long-term monitoring of LAI with minimum efforts (Tillack et al. 2014). Since last decades various optical, microwave and LiDAR satellites have been launched for global vegetation studies. Among them SPOT, Terra AQUA/MODIS satellites are available for studying the vegetation processes and to derive LAI information which, incorporating site-specific characteristics of vegetation (Yang et al. 2006). Local variation of vegetation is not captured in coarser resolution-based satellites. To know the site-specific characteristics of vegetation, LAI estimation is compulsory. Over the past three decades, to retrieve robust, reliable and accurate LAI, radiative transfer models were used. (Jacquemoud Stéphane and Baret 1990) has developed PROSPECT model to retrieve multidirectional reflectance and diffusion for the specific leaf. The combination of the leaf model with the canopy model (PROSAIL) provides reflectance and transmittance for the whole canopy. Generated RTM using PROSAIL model further can be used for inversion against optical (reflectance) measurements to retrieve LAI. These models require lot of optimization and expert computational effort. To overcome this problem various regression-based model has been introduced for LAI retrieval. Among them most commonly used indices were found to be normalized difference vegetation index (NDVI) and enhanced vegetation index (EVI) (Ma et al. 2022). Several studies have proven that these indices secured most closed relationships between the ground-based LAI and Vegetation Indices (Wang et al. 2005; Qiao et al. 2019; Tan et al. 2020).

Thus, crop simulation models aid in predicting crop growth and development by employing quantitative explanations of eco-physiological processes impacted by various environmental factors and crop management practices (Hodson and White 2010). These models can significantly aid in understanding climate change impacts and their interactions with varied crops (Revill et al. 2021; Yeşilköy and Şaylan 2021). This will thereby provide support in predicting the potential impacts of these changes on crop yield (Asseng et al. 2015). Crop modelling has been used primarily as a decision-making tool for crop management, but crop modelling, coupled with crop physiology and molecular biology, also could be useful in breeding programs (Slafer 2003). Since these models can make inferences about real systems, their application in agricultural systems currently represents a powerful resource for the evaluation of scenarios, management options and extrapolations of experimental results in space and time (Kumar P et al. 2019; Srivastava et al. 2021). They can also be used for academic purposes, research assistance, support systems, and management decision management as well as strategic planning analysis and management policies (Jones et al. 2003; Gupta, Gupta, et al. 2021).

The use of crop simulation models is dated back to the mid-1960s wherein simple mathematical equations were employed to depict crop processes (De Wit et al. 1995). Various models were then developed such as ARC-Wheat (Porter 1984), CERES-Wheat (Ritchie 1985) etc. Significant advances were achieved in crop modelling in 1990s where models incorporating climate change

impacts were built in understanding the projected impact of carbon dioxide concentration (Rosenzweig and Parry 1994). Few existing crop modelling platforms are Agricultural Production Systems Simulator (APSIM) (Keating et al. 2003), Environmental Policy Integrated Climate (EPIC) (Kiniry et al. 1995), Decision Support System for Agrotechnology Transfer (DSSAT) (Jones et al. 2003), CropSyst (Stöckle et al. 2003), Wageningen crop models and Simulator multidisciplinary pour Les Cultures Standards (STICS) (Brisson et al. 1998). Additionally, new methods merging single models with crop modelling platforms are also developed. Crop yield simulation using such crop simulation models is successfully achieved for different environments, biotic constraints, gene factors and climate change impacts and adaptations (Kheir et al. 2020; Maurya et al. 2020; Gupta, Singh, et al. 2021).

According to the previous studies (Kasampalis et al. 2018), crop models have the disadvantage of missing spatial information. The incorporation of remote sensing data with crop growth models provides a more accurate explanation of the crop's actual condition and various stages of the growing season (Challinor et al. 2009; Lobell and Burke 2010) over a large area. Increasing performance and continuous updating of hyperspectral technologies in terms of both spectral and spatial provide various studies and applications in vegetation mapping and crop modelling (Castaldi et al. 2016). A review was done by (Pascucci et al. 2020) on eleven international research studies, they have used different hyperspectral datasets for crop and vegetation modelling. Narrow contiguous bands of hyperspectral imaging have great potential for agriculture applications (Ali et al. 2016; Darvishzadeh et al. 2019; Xie et al. 2021). Therefore, the present work aimed at developing a model for crop stage simulation linked to LAI dynamics using hyperspectral data on a freely available R platform. This crop stage estimator uses hyperspectral spectroradiometer datasets and R interface to create, edit, and run simulations by taking Leaf area index (LAI) and crop stages as input parameters. To know the best LAI model performance and variability of LAI value over a larger area, mapping of LAI were done through AVIRIS-NG (Airborne Visible Near-Infrared Imaging Spectrometer - Next Generation) airborne datasets over test study area of Anand, Gujarat.

2. Study Area

Varanasi and Anand districts were selected as case study areas for model development and testing. The study was carried out in the agricultural fields of widely grown cereal crop namely wheat. Varanasi area is rich in crop productivity as it lies near the Gangetic belts. The sampling was mainly executed in the major regions covering more than 800 km^2 of the area. The average annual rainfall recorded in this region is 1056.4 mm per year. Wheat is the major cultivated crop during the rabi season and the area covered is 101.972 hectares (Rai; YADAV M et al. 2013). Varanasi district has a humid subtropical climate and is characterized by very hot and cold summers seasons. In the summer season, the temperature varies from 22°C to 46°C and below 5°C in the winter season. It follows the mixed cropping pattern and three cropping seasons (Kharif, Rabi and Zaid). Kharif crops are mainly shown between the month of June-July and harvested period is September, while rabi crops are sown in October- November and Zaid crops are in between the Rabi and Kharif seasons. Paddy crop covers the largest area in the Varanasi district (Kumari M et al. 2017; Nistor et al. 2020).

The second study site was selected namely Anand (Site Id 68) located in the Gujarat district which consists in the western part of India. The present site is part of the AVIRIS-NG India Campaign, which is a joint initiative of the Indian Space Research Organization (ISRO) and National Aeronautics and Space Administration (NASA). The geographical area covered by the study site is 22.6109° N - 72.9976°E and 22.5327°N - 73.8812°E, respectively. The study site is mainly covered by agricultural field crops like wheat, maize, sorghum etc. Wheat is the main dominating growing crop in the study area. Different types of soil such as black cotton, mixed red and black, are presented in the study area (Priyan 2015; Tripathy and Manjunath 2016). In the present study phase, 1 level 2 (Reflectance) AVIRIS-NG data was used for the LAI mapping.

3. The Crop stage model

3.1 Software & Input Requirements

The software used in the present study is R statistical software which is open-source software and can be freely downloaded using the link https://cran.r-project.org/mirrors.html. The mandatory package for this interface is the hsdar package which was successfully installed. A rigorous field sampling is needed to know the crop stage variations. Basic inputs to this software were multi-date hyperspectral reflectance data and ground truth data which were provided in CSV format. The step by step creation and development of this estimator has been described in **Figure 2**.

3.2 Ground truth data

The ground truth LAI was measured using LI-2200C Plant Canopy Analyzer (LI–COR®, Lincoln, NE, USA) instrument. It computes LAI from above and below the canopy, which is used to control canopy light interception at five angles using fisheyes which, provided in the sensor. This instrument is mostly known as the world standard instrument to measure LAI for every type of crop and canopies (Lena et al. 2016). Because of the most reliable and accurate measurement, this analyser has been used in many studies (Kanzler et al. 2019; Kandert et al. 2021; Yadav VP et al. 2021; Verma et al. 2022). In the present study, LAI was captured at different stages of wheat crop namely Tillering, Booting and Heading. Wheat crop stages were defined according to the study of Simmons (Simmons et al. 1985). Wheat crops at different growth stages in Varanasi agricultural fields are illustrated in **Figure 1 (a-c)**. The sampling was done during the Rabi season from mid-November 2019 to February 2020. Sampling was begun after 10 days of crop sowing, initial tillering to heading stage.

3.3 Hyperspectral Remote Sensing data

The Analytical spectral devices (ASD) FieldSpec4 spectroradiometer was used to capture reflectance data for the wheat crop at its tillering, booting and heading stages. It uses a fore-optic system to measure spectral reflectance and spectral radiance of any object and distribute it via a fibre optic bundle to a fixed diffraction grating spectrometer (Singh, Pandey, et al. 2020a). It has three different types of detectors to enable the recording of the spectra (Pandey et al. 2021). A silicon-photodiode-array for the visible near-infrared (350-1000 nm) region and thermoelectrically cooled InGaAs-photodiodes (Indium, Gallium, Arsenid) for each first short-wave infrared (1000-1800 nm) and second short wave infrared (1800-2500 nm). Hence, it stores band information ranging from 350-2500 nm. Spectral reflectance is the part or a fraction of incident electromagnetic (em) radiation that is reflected from any interface (Singh, Srivastava, et al. 2020a). The reflectance, when plotted as a function of wavelength, is known as the reflectance spectrum or spectral reflectance curve which is the end product of the device (Mac Arthur et al. 2012; Singh, Pandey, et al. 2020b; Srivastava et al. 2020). The spectral resolution varies from 3 nm in the very short wavelength regions and 10 nm in the farther regions of wavelengths. This ASD FieldSpec4 spectroradiometer records spectral information of 2151 bands (Janse et al. 2018; Singh, Pandey, et al. 2020b; Pandey et al. 2021).

Another hyperspectral data acquired from the airborne AVIRIS-NG flight over the study site Anand Gujarat was also used for LAI mapping. The necessary data was collected under the phase-1 campaign of AVIRIS-NG over the area of Anand, Gujrat site on 7th January 2016. An imaging spectrometer AVIRIS-NG consists of 425 narrow contiguous spectral bands range varies between 380-2510 nm at 5 nm spectral resolution with ground sampling distance from 4 to 8 m and flying altitude of 4-8 km (Singh, Srivastava, et al. 2020a). Availability of a large amount of spectral information, AVIRIS-NG data proves as a useful dataset for the land-cover distinction and

vegetation biophysical modelling (Bue et al. 2015). Ortho-rectified and atmospheric corrected reflectance L2 (Level 2) data was used for the LAI mapping. Detailed information can be seen in **Table 1.**

3.4 Crop Stage Estimator

The research focuses on the development of a user-friendly environment where various types of hyperspectral analysis can be performed just by providing input data. In order to handle hyperspectral data, users need a large volume of space, high performing computer with good knowledge of programming languages to analyse hyperspectral measurements. Development of this model on freely available R software and a complete environment for processing provides a better solution for non-programming users to handle hyperspectral data. This environment is applicable for agricultural region and for wheat crop to estimate LAI information.

Crop Stage Estimator is a novel model in the field of crop modelling and it possesses certain salient features that are essentially required for fast processing of the datasets can be intgertaed with other systems. This model is easy to implement and also provides step by step user-friendly process to know the crop stages linked to the LAI using hyperspectral data on a freely available R platform. It comprises various functions which can be used to create, edit, and run simulations by taking Leaf area index (LAI), crop stages and hyperspectral data as input parameters and finally analysing outputs from R. The flow chart depicting the present study can be seen in **Figure 2**. The performances of Crop Stage Estimator was tested by running this model using developed example flow for Varanasi wheat crop. Set example workflow was used with Leaf Area Index (LAI) and Analytical Spectral Devices (ASD) FieldSpec 4 Hi-Res Spectroradiometer hyperspectral reflectance data collected for wheat (Triticum aestivum L.) crop at different growth stages (heading, tillering and booting) growing in the agricultural fields of Varanasi. Workflow provides the code that can be used for modifying values in input data files, running simulations, reading simulated output, and creating publication-quality visualizations of observed and simulated data. Results of this performance check demonstrated that how the crop stage estimator can be used to perform various crop stage analyses and processing in a single platform. It further demonstrated the validation of the crop model for developing crop stage variation between ground and modelled crop parameters using a crop stage estimator.

A simulation model developed in the present study is given the name “Crop Stage Estimator”. This model runs under the R environment. It provides a user-friendly interface to analyze hyperspectral data. Various steps involved for development and running this model under R environment includes (1) Input of multidate hyperspectral reflectance data captured by ASD-Spectroradiometer instrument in CSV (comma-separated values) format according to wheat crop stages such as Tillering, Heading and Booting (2) In the next step, to understand the difference between crop stages, crop stage-wise generation of the spectral profile has been created by using the hyperspectral data (3) Provided input data was further used for the development of vegetation indices at different crop growth stages using vegindex function of hsdar package in R (Lehnert et al. 2018) which aids in calculating all available vegetation indices as well as user-defined indices can be developed after providing the customised formula (4) In next step, identification and selection of optimum LAI model based on the best correlation values between modelled and ground- based parameter can be generated (5) In order to know the model robustness, statistical performance has been performed between best LAI modelled values and ground-based validation data. (6) Linear plot development to understand the stage-wise crop growth variations (7) Finally, the LAI mapping using the best LAI model has been performed by using the AVIRIS-NG data.

3.5 Validation and Accuracy assessment

To know the model efficiency and robustness, validation was done on both study areas namely, Varanasi and Anand Gujarat. Data was portioned into two categories. From the total collected ground data, 70% were used for model calibration and 30% for model validation. A Scatter plot was plotted to check the performance of the model by comparing statistical parameters viz. Bias, RMSE and correlation between Ground LAI and simulated LAI.

The correlation coefficient (r) calculated using this equation

$$r = \frac{n\sum xy - (\sum x)(\sum y)}{\sqrt{\left[n\sum x^2 - (\Sigma x)^2\right]\left[n\sum y^2 - (\Sigma y^2)\right]}} \quad (7)$$

where x and y are the ground-based and estimated measurements respectively, whereas n is the total number of observations.

RMSE (Root Mean Square Error) calculated using this equation

$$RMSE = \sqrt{\left(\frac{1}{n}\sum_{i=1}^{n}\left[y_i - x_i\right]^2\right)} \quad (8)$$

The absolute Bias is calculated to understand the positive or negative deviation from the actual values. Bias calculated using the following equation;

$$Bias = (\bar{y} - \bar{x}) \quad (9)$$

where $\bar{x}$ is the mean of ground-based measurements and $\bar{y}$ is the mean of estimated measurement (Singh et al. 2021). The layout of the example workflow is shown in Figure 3.

4. Results and Discussions

4.1 Results

4.1.1. LAI dynamics with different crop stages

Properly quantification of LAI is very difficult, concerning ecological, varietal factors and temporal variability. Various methods have been established for the estimation of LAI and also yielded good results, but due to the unavailability of large time-series parameters proper coefficients are not developed for LAI monitoring (Bin et al. 2010). In the present study, crop estimator was developed for the retrieval of LAI and also to obtain crop growth stages through hyperspectral spectroradiometer reflectance data and ground truth crop parameter viz. LAI data for the wheat crop at different growth stages such as Tillering, Booting and Heading.

Variations in LAI values at different stages of wheat crop grown in Varanasi were observed and shown in **Figure 4**. To understand the overall distribution of the datasets and the box and whisker diagrams were generated. These box and whisker diagrams represent the distribution of data in terms of maximum, minimum, median, and both the upper and lower quartile in a single plot. Minimum and maximum LAI values for Tillering stage were observed as 0.12 and 0.71 respectively whereas for the booting stage of wheat it was found as 1.25 and 1.81 respectively. For the Heading stage of the wheat crop minimum and maximum LAI values noted were 2.21 and 3.93 respectively. LAI

varies with seasonal changes according to plant activity and highest LAI found in dense canopies and lowest in early-stage or leaves senescence maturity stage (Maass et al. 1995; Bedigian and evolution 2003).

4.1.2. Spectral response with changing canopy conditions

Stage wise spectral library for wheat crop growing in Varanasi is depicted in **Figure 5**. It has spectral variability at various stages that can be used for crop stage discrimination. The highest peak in reflectance was observed in NIR (Near -Infrared) region during Tillering, which was noted as 75%. Minimum reflectance value i.e. 58% was observed for the Heading stage of the wheat crop. Spectral variations among curves are mainly occurred due to spectral differences in crop growth stages. The lowest reflectance values were observed in the tillering stage because reflectance values are mainly influenced by soil and low biomass. Maximum reflectance in jointing or heading stage due to highest values of green leaf area index and high scattering of solar radiation in NIR (Moreira et al. 1999). Further, these reflectance values were used as the inputs for the calculation of vegetation indices.

4.1.3. *Assessment of indices and LAI generated from Crop stage estimator*

All available more than hundred already developed hyperspectral vegetation indices were calculated for wheat crop growing at different stages. Correlations between calculated indices and ground LAI data for different stages of wheat were established and five best-correlated indices for each stage were determined and shown in the scatterplot **Figure 6 (a-c)**. The five best indices identified for tillering stage are NDVI (Normalized difference vegetation index), PARS (Ratio Analysis of Reflectance Spectra), PSSR (Pigment Specific Simple Ratio), SRPI (Simple ratio Pigment Index) and GDVI (Generalized Difference vegetation Index). NDVI was identified as the best among the five indices which showed the greatest correlation with LAI at tillering stage (r = 0.66). For the booting stage, five top correlated indices are NDVI, GDVI, MSAVI (Modified Soil-Adjusted Vegetation Index), OSAVI (Optimized Soil-Adjusted Vegetation Index) and SR (Simple ratio). Even at the booting stage, NDVI was observed to be the best-correlated vegetation index with LAI with an r-value of 0.59. The top five best indices are GDVI, NDVI, MSAVI, OSAVI and SR. Among them, mNDVI (Modified Normalized difference vegetation index) was found to be the best-correlated vegetation index to LAI at the heading stage (r = 0.57).

The LAI models established using best relations between LAI and vegetation index at respective stages were further used for estimating LAI. The best LAI model for tillering, booting and heading stage were displayed using multiple linear regression plots. Among them, vegetation indices at tillering stage showed a highly significant relation between ground LAI and vegetation index. **Figure 7.** Line diagram was plotted to observe variations in ground and modelled LAI at different stages. The dotted red line corresponds to the model predictions, while the dotted blue line corresponds to the ground truth variation. The same increasing pattern was observed from tillering to heading stage for both grounds and modelled LAI. According to the linear plot, it is visible ground and modelled LAI observed a close relationship for all growth stages **Figure 8**. Among all stages tillering stage model was found to be the best optimum model for LAI retrieval. Using best optimum model validation was performed which, showed a highly significant relation between ground and modelled LAI with r = 0.98, RMSE = 0.20, and Bias = 0.12 (**Figure 9).**

4.1.4. LAI mapping

According to the overall results of hyperspectral vegetation indices, NDVI indices-based model at the tillering stage was proved to be the best optimum model for generation of LAI values. Further, this best model was used as an input for generating LAI map using the AVIRIS-NG airborne dataset

of Anand, Gujrat. Raw rectified phase -1, level 2 image and LAI map of AVIRIS-NG can be seen in **Figure 10**. Zoomed area of both scenes also can be seen on the right side of the images. The range of LAI was varying among 0.78 – 0.89. LAI values were observed similar to the range of LAI values which was estimated at sampling study sites of Varanasi at tillering stage. This shows that the model is quite effective and the further outcome can be used for other agricultural areas and crop growth, monitoring and assessment.

4.2. Discussions

Previous studies examined the variations in wheat crop stages, which highlighted an increasing pattern in LAI for initial crop development stages for mid-season and decreasing LAI trend for a late-season (maturity stage) (Kumar V et al. 2013). Another research determining stage-wise LAI variation is available wherein an increasing trend in LAI was observed due to the increased number of tillers (stages) and size of successive leaves (Rahman et al. 2014). (Kumari P et al. 2009) performed field experiment at Ranchi, Jharkhand to understand the response of the wheat crop. In their study, experiment was done according to phenological stages of crop such as emergence, tillering, jointing, booting, flowering, milking and maturity. An increasing trend in LAI was observed till the flowering stage and decreasing patterns were observed for milking and maturity stages. The observed output of the LAI variation in the present study corresponds with the previous studies since it follows the same LAI pattern at different crop stages. Various studies have been conducted to develop crop growth models for the estimation of the most influential, variable of crop growth named Leaf Area Index (Daughtry et al. 1992; Jacquemoud S et al. 1996; Fassnacht et al. 1997). Among them, a study was conducted by (Yuan et al. 2017) Jiaxiang County for the investigation of an optimal model for soybean crop for all growth periods using simple random sampling and stratified type sampling methods.

Several machine learning such as random forest, artificial neural network and support vector machine regression models were compared with a partial least-squares regression (PLS) model for the estimation of LAI (Goel 1988; Verhoef 1998). Among them, ANN model yielded the highest accuracy with R^2 0.452 and RMSE 0.106 respectively (Li X et al. 2014). Another study was conducted at Greenbelt Farm of Agriculture and Agri-Food Canada for LAI estimation. PROSPECT and SAILH radiative transfer models were used to simulate the range of canopy reflectance and understand the variations of LAI for the wheat crop (Haboudane et al. 2008). To estimate the leaf area index (LAI) several existing vegetation indices, such as Normalized Difference Vegetation Index (NDVI), Renormalized Difference Vegetation Index (RDVI), Modified Simple Ratio (MSR), Soil-Adjusted Vegetation Index (SAVI), Soil and Atmospherically Resistant Vegetation Index (SAARVI) and modified triangular vegetation index (MTVI) were used (Li F et al. 2014). Among them, MTVI proved to be the best predictor of green LAI. MTVI index showed a significant relation with the ground LAI and observed performance values in terms of R^2 and RMSE (0.54, 0.85) for wheat crop respectively (Haboudane et al. 2004). According to the performance analysis of previous studies, the current study outperforms and thus the estimator developed through this study can be used for LAI mapping.

6. Conclusion

In this study, a hyperspectral-based crop stage estimator interface has been developed on freely available R software. To analyze the performance, an example workflow was created for wheat at different crop growth stages. The presented interface can perform simple steps which makes it robust and user friendly. It also has quick processability of larger datasets. This interface will provide a common platform for the generation of the spectral library, calculation of vegetation indices, development of best LAI model and its mapping. This common platform will be also helpful for non-

programming users due to simple layout and working. This novel model extends the basic tools which on combining with other R packages will facilitate developing robust, reproducible, scientific modelling workflows. Further crop stage estimator can be used to understand crop stage variations by integrating other crops biophysical (Biomass, Plant height, Root depth) and biochemical (Chlorophyll) parameters.

Acknowledgement

The first and corresponding author would like to thank SAC, ISRO for providing necessary support for this research under the AVIRIS-NG scheme. The authors also would like to express their sincere thanks to Banaras Hindu University, Varanasi for providing the necessary support.

Conflict of interest

There is no conflict of interest

References

Crop growth modelling in India: past, present and future. Potato, global research & development Proceedings of the Global Conference on Potato, New Delhi, India, 6-11 December, 1999: Volume 2; 2002: Indian Potato Association.

Ahmad S, Pandey AC, Kumar A, Lele NVJAG. 2021. Potential of hyperspectral AVIRIS-NG data for vegetation characterization, species spectral separability, and mapping.1-12.

Ali AM, Skidmore AK, Darvishzadeh R, van Duren I, Holzwarth S, Mueller J. 2016. Retrieval of forest leaf functional traits from HySpex imagery using radiative transfer models and continuous wavelet analysis. ISPRS journal of photogrammetry remote sensing. 122:68-80.

Anand A, Malhi RKM, Srivastava PK, Singh P, Mudaliar AN, Petropoulos GP, Kiran GS. 2021. Optimal band characterization in reformation of hyperspectral indices for species diversity estimation. Physics Chemistry of the Earth, Parts A/B/C.103040.

Asseng S, Zhu Y, Wang E, Zhang W. 2015. Crop modeling for climate change impact and adaptation. Crop physiology. Elsevier; p. 505-546.

Bedigian DJGr, evolution c. 2003. Evolution of sesame revisited: domestication, diversity and prospects. 50(7):779-787.

Bin Z, Ming Z, Zhiqiang D, Jianguo L, Chuanyong C, Rui S. 2010. Establishment and test of LAI dynamic simulation model for high yield population.

Bouman B, Van Keulen H, Van Laar H, Rabbinge R. 1996. The 'School of de Wit'crop growth simulation models: a pedigree and historical overview. Agricultural systems. 52(2-3):171-198.

Simulation of potato-based cropping systems. Potato, global research & development Proceedings of the Global Conference on Potato, New Delhi, India, 6-11 December, 1999: Volume 2; 2002: Indian Potato Association.

Brisson N, Mary B, Ripoche D, Jeuffroy M-H, Ruget F, Nicoullaud B, Gate P, Devienne-Barret F, Antonioletti R, Dürr C. 1998. STICS: a generic model for the simulation of crops and their water and nitrogen balances. I. Theory and parameterization applied to wheat and corn. Agronomie. 18(5-6):311-346.

Bue BD, Thompson DR, Eastwood M, Green RO, Gao B-C, Keymeulen D, Sarture CM, Mazer AS, Luong HHJIToG, Sensing R. 2015. Real-time atmospheric correction of AVIRIS-NG imagery. 53(12):6419-6428.

Castaldi F, Palombo A, Santini F, Pascucci S, Pignatti S, Casa R. 2016. Evaluation of the potential of the current and forthcoming multispectral and hyperspectral imagers to estimate soil texture and organic carbon. Remote Sensing of Environment. 179:54-65.

Challinor AJ, Ewert F, Arnold S, Simelton E, Fraser E. 2009. Crops and climate change: progress, trends, and challenges in simulating impacts and informing adaptation. Journal of experimental botany. 60(10):2775-2789.

Chapin FS, Woodwell GM, Randerson JT, Rastetter EB, Lovett GM, Baldocchi DD, Clark DA, Harmon ME, Schimel DS, Valentini RJE. 2006. Reconciling carbon-cycle concepts, terminology, and methods. 9(7):1041-1050.

Darvishzadeh R, Skidmore A, Abdullah H, Cherenet E, Ali A, Wang T, Nieuwenhuis W, Heurich M, Vrieling A, O'Connor B. 2019. Mapping leaf chlorophyll content from Sentinel-2 and RapidEye data in spruce stands using the invertible forest reflectance model. International Journal of Applied Earth Observation Geoinformation. 79:58-70.

Daughtry C, Gallo K, Goward S, Prince S, Kustas WJRSoE. 1992. Spectral estimates of absorbed radiation and phytomass production in corn and soybean canopies. 39(2):141-152.

De Wit CC, Olsson H, Astrom KJ, Lischinsky P. 1995. A new model for control of systems with friction. IEEE Transactions on automatic control. 40(3):419-425.

Fang H, Zhang Y, Wei S, Li W, Ye Y, Sun T, Liu WJRSoE. 2019. Validation of global moderate resolution leaf area index (LAI) products over croplands in northeastern China. 233:111377.

Fassnacht KS, Gower ST, MacKenzie MD, Nordheim EV, Lillesand TMJRsoe. 1997. Estimating the leaf area index of north central Wisconsin forests using the Landsat Thematic Mapper. 61(2):229-245.

Goel NSJRsr. 1988. Models of vegetation canopy reflectance and their use in estimation of biophysical parameters from reflectance data. 4(1):1-212.

Gupta A, Gupta M, Srivastava PK, Sen A, Singh RK. 2021. Subsurface nutrient modelling using finite element model under Boro rice cropping system. Environment, Development Sustainability.1-22.

Gupta A, Singh P, Srivastava PK, Pandey MK, Anand A, Chandra Sekar K, Shanker K. 2021. Development of hyperspectral indices for anti-cancerous Taxol content estimation in the Himalayan region. Geocarto International.(just-accepted):1-14.
Haboudane D, Miller JR, Pattey E, Zarco-Tejada PJ, Strachan IBJRsoe. 2004. Hyperspectral vegetation indices and novel algorithms for predicting green LAI of crop canopies: Modeling and validation in the context of precision agriculture. 90(3):337-352.
Haboudane D, Tremblay N, Miller JR, Vigneault PJIToG, Sensing R. 2008. Remote estimation of crop chlorophyll content using spectral indices derived from hyperspectral data. 46(2):423-437.
Hodson D, White J. 2010. GIS and crop simulation modelling applications in climate change research. Climate change crop production Wallingford, UK: CABI Publishers.245-262.
Jacquemoud S, Baret FJRsoe. 1990. PROSPECT: A model of leaf optical properties spectra. 34(2):75-91.
Jacquemoud S, Ustin S, Verdebout J, Schmuck G, Andreoli G, Hosgood BJRsoe. 1996. Estimating leaf biochemistry using the PROSPECT leaf optical properties model. 56(3):194-202.
Standard Spectral Reflectance Measurements for ASD FieldSpec Spectroradiometer. 2018 Fifth International Conference on Parallel, Distributed and Grid Computing (PDGC); 2018: IEEE.
Jones JW, Hoogenboom G, Porter CH, Boote KJ, Batchelor WD, Hunt L, Wilkens PW, Singh U, Gijsman AJ, Ritchie JT. 2003. The DSSAT cropping system model. European journal of agronomy. 18(3-4):235-265.
Kandert S, Kreft H, DiManno N, Uowolo A, Cordell S, Ostertag RJPS. 2021. Influence of Light and Substrate Conditions on Regeneration of Native Tree Saplings in the Hawaiian Lowland Wet Forest1. 75(1):107-127.
Kanzler M, Böhm C, Mirck J, Schmitt D, Veste MJAs. 2019. Microclimate effects on evaporation and winter wheat (Triticum aestivum L.) yield within a temperate agroforestry system. 93(5):1821-1841.
Kasampalis DA, Alexandridis TK, Deva C, Challinor A, Moshou D, Zalidis G. 2018. Contribution of remote sensing on crop models: a review. Journal of Imaging. 4(4):52.
Keating BA, Carberry PS, Hammer GL, Probert ME, Robertson MJ, Holzworth D, Huth NI, Hargreaves JN, Meinke H, Hochman Z. 2003. An overview of APSIM, a model designed for farming systems simulation. European journal of agronomy. 18(3-4):267-288.
Kheir AMS, Ding Z, Ali MGM, Feike T, Abdelaal AIN, Elnashar A. 2020. Wheat Crop Modelling for Higher Production. Systems Modeling. Springer; p. 179-202.
Kiniry JR, Williams JR, Major D, Izaurralde R, Gassman PW, Morrison M, Bergentine R, Zentner R. 1995. EPIC model parameters for cereal, oilseed, and forage crops in the northern Great Plains region. Canadian Journal of Plant Science. 75(3):679-688.

Kumar P, Prasad R, Choudhary A, Gupta D, Mishra V, Vishwakarma A, Singh A, Srivastava P. 2019. Comprehensive evaluation of soil moisture retrieval models under different crop cover types using C-band synthetic aperture radar data. Geocarto International. 34(9):1022-1041.
Kumar V, Kumari M, Saha SK. 2013. Leaf area index estimation of lowland rice using semi-empirical backscattering model. Journal of Applied Remote Sensing. 7(1):073474.
Kumari M, Singh O, Meena DC. 2017. Optimising Cropping Pattern in Eastern Uttar Pradesh Using Sen's Multi Objective Programming Approach. Agricultural Economics Research Review. 30(347-2018-2897):285-295.
Kumari P, Wadood A, Singh R, Kumar R. 2009. Response of wheat crop to different thermal regimes under the agroclimatic conditions of Jharkhand. Journal of Agrometeorology. 11(1):85-88.
Lehnert L, Meyer H, Bendix. 2018. Hsdar: Manage. Analyse Simulate Hyperspectral Data in R.
Lena B, Folegatti M, Francisco J, Santos O, Andrade IJJoA. 2016. Performance of LAI-2200 plant canopy analyzer on Leaf Area Index of jatropha nut estimation. 15(4):191-197.
Li F, Mistele B, Hu Y, Chen X, Schmidhalter UJEJoA. 2014. Reflectance estimation of canopy nitrogen content in winter wheat using optimised hyperspectral spectral indices and partial least squares regression. 52:198-209.
Li X, Zhang Y, Bao Y, Luo J, Jin X, Xu X, Song X, Yang GJRS. 2014. Exploring the best hyperspectral features for LAI estimation using partial least squares regression. 6(7):6221-6241.
Lobell DB, Burke MB. 2010. On the use of statistical models to predict crop yield responses to climate change. Agricultural forest meteorology. 150(11):1443-1452.
Ma Y, Zhang Q, Yi X, Ma L, Zhang L, Huang C, Zhang Z, Lv X. 2022. Estimation of Cotton Leaf Area Index (LAI) Based on Spectral Transformation and Vegetation Index. Remote Sensing. 14(1).
Maass J, Vose JM, Swank WT, Martínez-Yrízar AJFE, Management. 1995. Seasonal changes of leaf area index (LAI) in a tropical deciduous forest in west Mexico. 74(1-3):171-180.
Mac Arthur A, MacLellan CJ, Malthus T. 2012. The fields of view and directional response functions of two field spectroradiometers. IEEE transactions on geoscience remote sensing. 50(10):3892-3907.
Malhi RKM, Pandey MK, Anand A, Srivastava PK, Petropoulos GP, Singh P, Sandhya Kiran G, Bhattarcharya B. 2020. Band selection algorithms for foliar trait retrieval using AVIRIS-NG: a comparison of feature based attribute evaluators. Geocarto International.1-17.
Maurya NK, Singh P, Srivastava PK. 2020. Assessment of Hyperspectral Indices-Based Chlorophyll Models for Maize Crop. Bulletin of Environmental Scientific Researc. 9(1):1-4.
Mbow H-OP, Reisinger A, Canadell J, O'Brien P. 2017. Special Report on climate change, desertification, land degradation, sustainable land management, food security, and greenhouse gas fluxes in terrestrial ecosystems (SR2). J Ginevra, IPCC.

Moreira MA, Angulo Filho R, Rudorff BFTJSA. 1999. Radiation use efficiency and harvest index for wheat undre drought stress at different growth stages. 56(3):597-603.
Nistor MM, Rai PK, Dugesar V, Mishra VN, Singh P, Arora A, Kumra VK, Carebia IA. 2020. Climate change effect on water resources in Varanasi district, India. Meteorological Applications. 27(1):e1863.
Pandey PC, Pandey MK, Gupta A, Singh P, Srivastava PK. 2021. Spectroradiometry: types, data collection, and processing. Advances in Remote Sensing for Natural Resource Monitoring.9-27.
Park S, Hwang C, Vlek P. 2005. Comparison of adaptive techniques to predict crop yield response under varying soil and land management conditions. Agricultural Systems. 85(1):59-81.
mPascucci S, Pignatti S, Casa R, Darvishzadeh R, Huang W. 2020. Special Issue "Hyperspectral Remote Sensing of Agriculture and Vegetation". Multidisciplinary Digital Publishing Institute.
Porter J. 1984. A model of canopy development in winter wheat. The Journal of Agricultural Science. 102(2):383-392.
Priyan KJAP. 2015. Spatial and temporal variability of rainfall in Anand District of Gujarat State. 4:713-720.
Qiao K, Zhu W, Xie Z, Li PJRS. 2019. Estimating the seasonal dynamics of the leaf area index using piecewise LAI-VI relationships based on phenophases. 11(6):689.
Rahman M, Islam M, Islam M, Karim M. 2014. Dry matter accumulation, leaf area index and yield responses of wheat under different levels of nitrogen. Bangladesh Journal of Agriculturist. 7(1):27-32.
Rai A. A STUDY ON e-READINESS OF KRISHI VIGYAN KENDRA FUNCTIONARIES IN UTTAR PRADESH. Institute of Agricultural Sciences, Banaras Hindu University.
Revill A, Myrgiotis V, Florence A, Hoad S, Rees R, MacArthur A, Williams M. 2021. Combining process modelling and LAI observations to diagnose winter wheat nitrogen status and forecast yield. Agronomy. 11(2):314.
Ritchie J. 1985. A user-orientated model of the soil water balance in wheat. Wheat growth and modelling. Springer; p. 293-305.
Rosenzweig C, Parry ML. 1994. Potential impact of climate change on world food supply. Nature. 367(6459):133-138.
Shukla P, Skea J, Calvo Buendia E, Masson-Delmotte V, Pörtner H, Roberts D, Zhai P, Slade R, Connors S, Van Diemen R. 2019. IPCC, 2019: Climate Change and Land: an IPCC special report on climate change, desertification, land degradation, sustainable land management, food security, and greenhouse gas fluxes in terrestrial ecosystems.

Silva JV, Reidsma P, Baudron F, Jaleta M, Tesfaye K, van Ittersum MK. 2021. Wheat yield gaps across smallholder farming systems in Ethiopia. Agronomy for Sustainable Development. 41(1):1-16.
Simmons S, Oelke E, Anderson P. 1985. Growth and development guide for spring wheat.
Singh P, Pandey PC, Petropoulos GP, Pavlides A, Srivastava PK, Koutsias N, Deng KAK, Bao Y. 2020a. 8 - Hyperspectral remote sensing in precision agriculture: present status, challenges, and future trends. In: Pandey PC, Srivastava PK, Balzter H et al., editors. Hyperspectral Remote Sensing. Elsevier; p. 121-146.
Singh P, Pandey PC, Petropoulos GP, Pavlides A, Srivastava PK, Koutsias N, Deng KAK, Bao Y. 2020b. Hyperspectral remote sensing in precision agriculture: Present status, challenges, and future trends. Hyperspectral remote sensing. Elsevier; p. 121-146.
Singh P, Srivastava PK, Malhi RKM, Chaudhary SK, Verrelst J, Bhattacharya BK, Raghubanshi AS. 2020a. Denoising AVIRIS-NG data for generation of new chlorophyll indices. IEEE Sensors Journal. 21(5):6982-6989.
Singh P, Srivastava PK, Malhi RKM, Chaudhary SK, Verrelst J, Bhattacharya BK, Raghubanshi AS. 2020b. Denoising AVIRIS-NG data for generation of new chlorophyll indices. IEEE Sensors Journal. 21(5):6982-6989.
Singh P, Srivastava PK, Mall R. 2021. Estimation of potential evapotranspiration using INSAT-3D satellite data over an agriculture area. Agricultural Water Management. Elsevier; p. 143-155.
Slafer G. 2003. Genetic basis of yield as viewed from a crop physiologist's perspective. Annals of Applied Biology. 142(2):117-128.
Srivastava PK, Malhi RKM, Pandey PC, Anand A, Singh P, Pandey MK, Gupta A. 2020. Revisiting hyperspectral remote sensing: Origin, processing, applications and way forward. Hyperspectral remote sensing. Elsevier; p. 3-21.
Srivastava PK, Singh P, Pandey V, Gupta M. 2021. Development of android application for visualisation of soil water demand. Agricultural Water Management. Academic Press; p. 375-389.
Stöckle CO, Donatelli M, Nelson R. 2003. CropSyst, a cropping systems simulation model. European journal of agronomy. 18(3-4):289-307.
Tan C-W, Zhang P-P, Zhou X-X, Wang Z-X, Xu Z-Q, Mao W, Li W-X, Huo Z-Y, Guo W-S, Yun FJSr. 2020. Quantitative monitoring of leaf area index in wheat of different plant types by integrating NDVI and Beer-Lambert law. 10(1):1-10.
Tao H, Feng H, Xu L, Miao M, Long H, Yue J, Li Z, Yang G, Yang X, Fan LJS. 2020. Estimation of crop growth parameters using UAV-based hyperspectral remote sensing data. 20(5):1296.
Tillack A, Clasen A, Kleinschmit B, Förster MJRSoE. 2014. Estimation of the seasonal leaf area index in an alluvial forest using high-resolution satellite-based vegetation indices. 141:52-63.

Assessing wheat residue cover with hyperspectral remote sensing. Multispectral, Hyperspectral, and Ultraspectral Remote Sensing Technology, Techniques and Applications VI; 2016: International Society for Optics and Photonics.
Verhoef W. 1998. Theory of radiative transfer models applied in optical remote sensing of vegetation canopies. Wageningen University and Research.
Verma B, Prasad R, Srivastava PK, Yadav SA, Singh P, Singh RJC, Agriculture Ei. 2022. Investigation of optimal vegetation indices for retrieval of leaf chlorophyll and leaf area index using enhanced learning algorithms. 192:106581.
Wang Q, Adiku S, Tenhunen J, Granier AJRsoe. 2005. On the relationship of NDVI with leaf area index in a deciduous forest site. 94(2):244-255.
Wolday K, Hruy G. 2015. A review: performance evaluation of crop simulation model (APSIM) in prediction crop growth, development and yield in semi-arid tropics. Journal of Natural Sciences Research. 5(21):34-39.
Xie R, Darvishzadeh R, Skidmore AK, Heurich M, Holzwarth S, Gara TW, Reusen I. 2021. Mapping leaf area index in a mixed temperate forest using Fenix airborne hyperspectral data and Gaussian processes regression. International Journal of Applied Earth Observation Geoinformation. 95:102242.
YADAV M, SINGH R, PATEL C. 2013. Rainfall Characteristics Analysis for Rice Based Cropping System at Varanasi, Uttar Pradesh. Journal of Agricultural Physics. 13(2):186-192.
Yadav VP, Prasad R, Bala RJGI. 2021. Leaf area index estimation of wheat crop using modified water cloud model from the time-series SAR and optical satellite data. 36(7):791-802.
Yang W, Tan B, Huang D, Rautiainen M, Shabanov NV, Wang Y, Privette JL, Huemmrich KF, Fensholt R, Sandholt IJIToG et al. 2006. MODIS leaf area index products: From validation to algorithm improvement. 44(7):1885-1898.
Yeşilköy S, Şaylan L. 2021. Yields and water footprints of sunflower and winter wheat under Different Climate Projections. Journal of Cleaner Production. 298:126780.
Yu RJEM. 2020. An improved estimation of net primary productivity of grassland in the Qinghai-Tibet region using light use efficiency with vegetation photosynthesis model. 431:109121.
Yuan H, Yang G, Li C, Wang Y, Liu J, Yu H, Feng H, Xu B, Zhao X, Yang XJRS. 2017. Retrieving soybean leaf area index from unmanned aerial vehicle hyperspectral remote sensing: Analysis of RF, ANN, and SVM regression models. 9(4):309.

[a] Tillering [b] Booting [c] Heading

Figure 1. (a-c) Different stages wheat crop over agriculture field of Varanasi

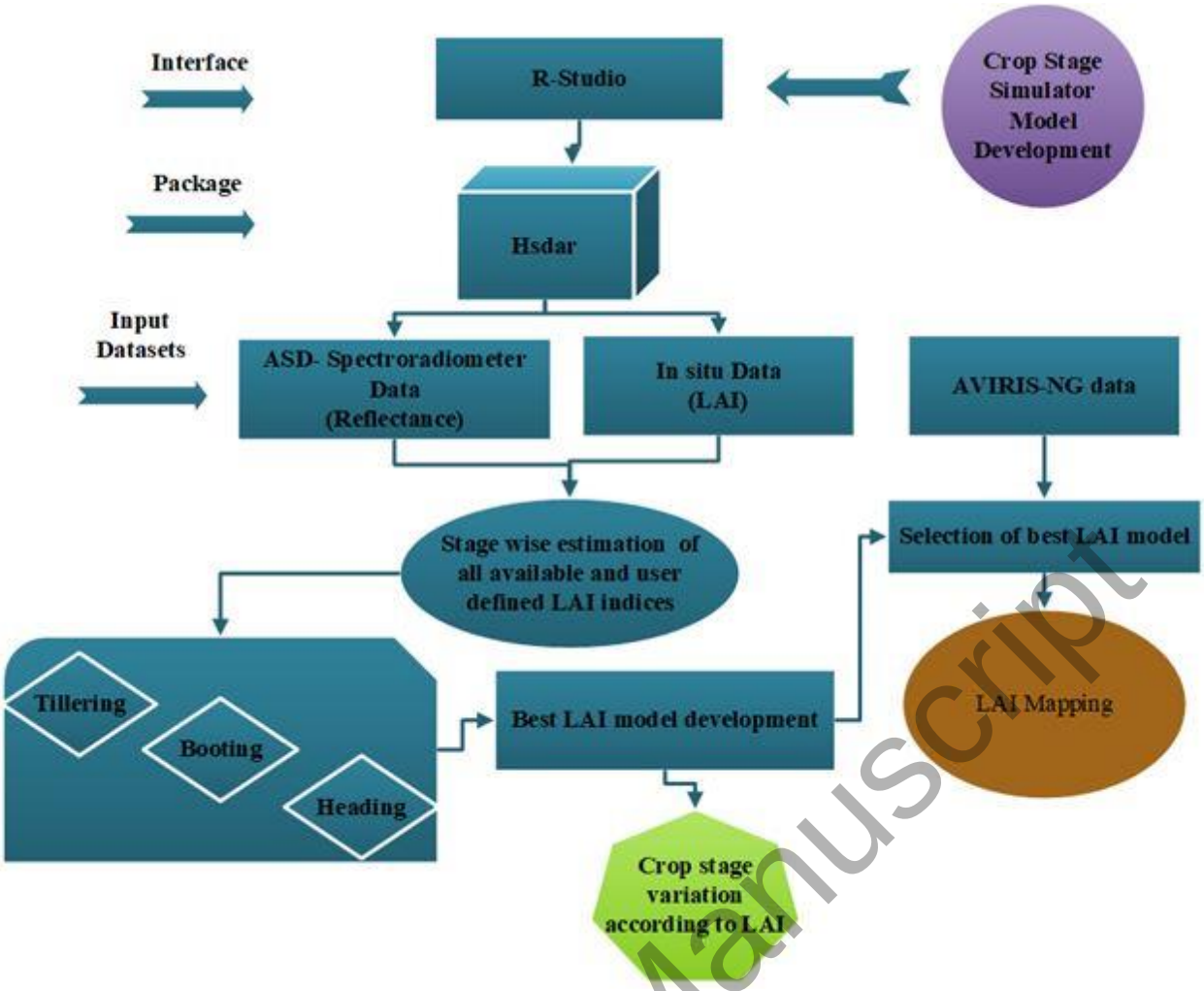

Figure 2. Flow diagram crop stage simulation model

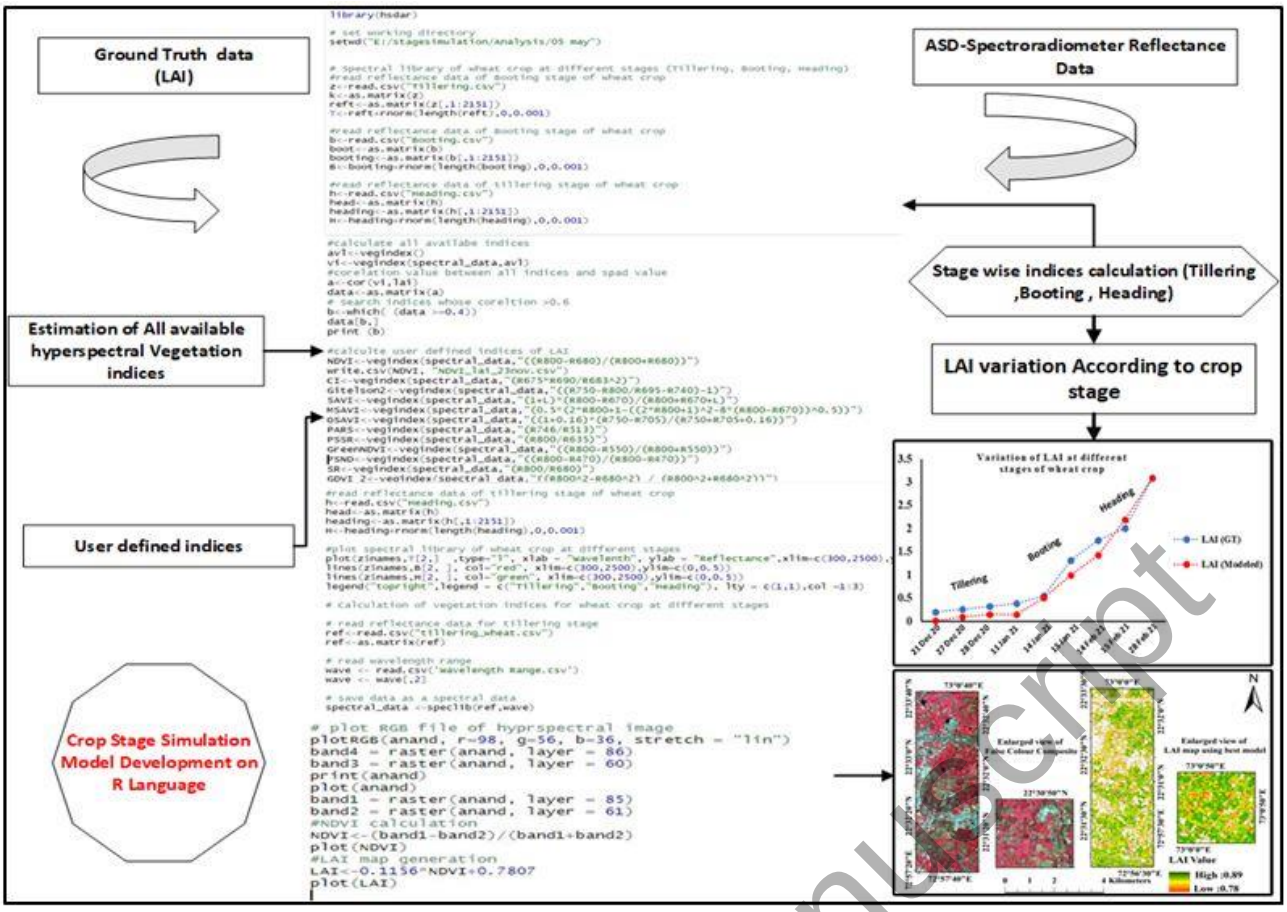

Figure 3. Example workflow of Crop Stage Simulator

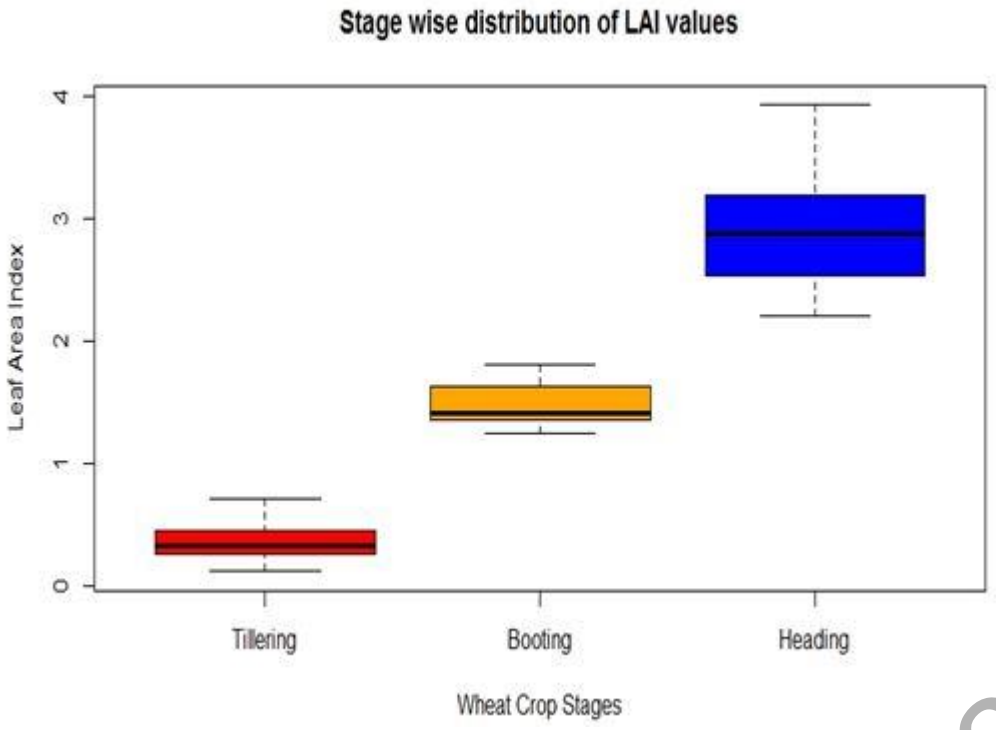

Figure 4. Stage wise LAI distribution

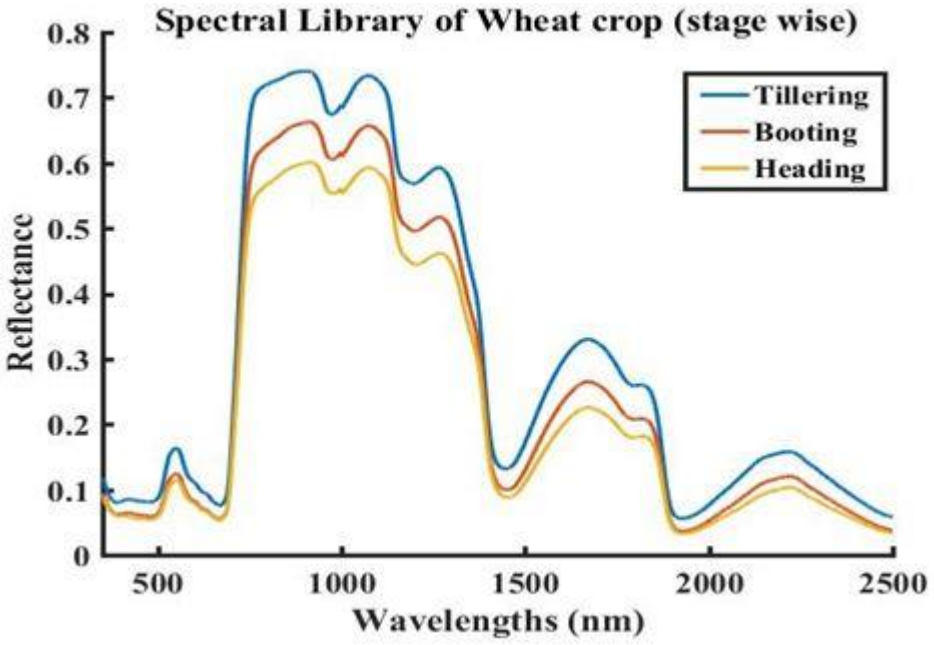

Figure 5. Spectral Library of the wheat crop at different stages over agriculture field of Varanasi

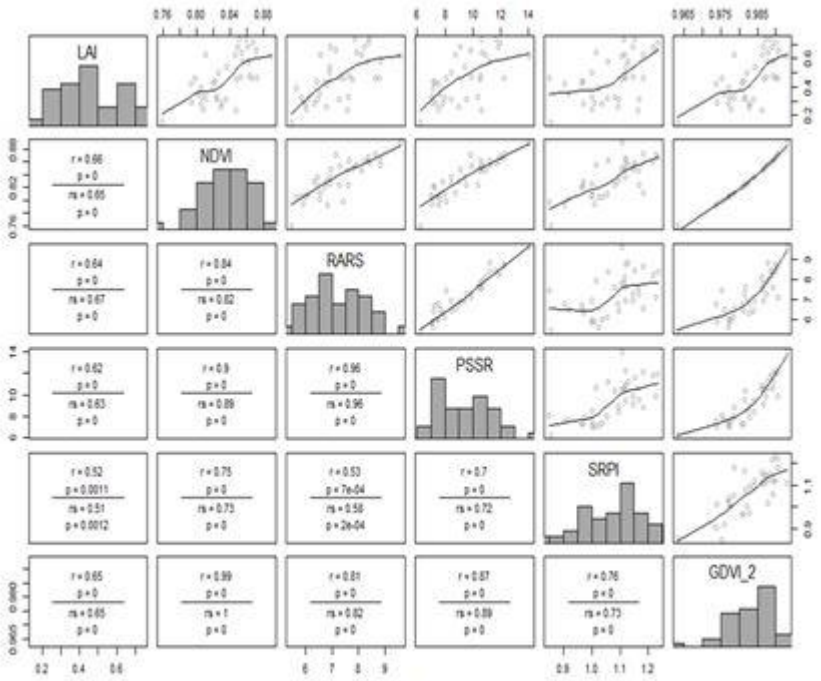

[a]

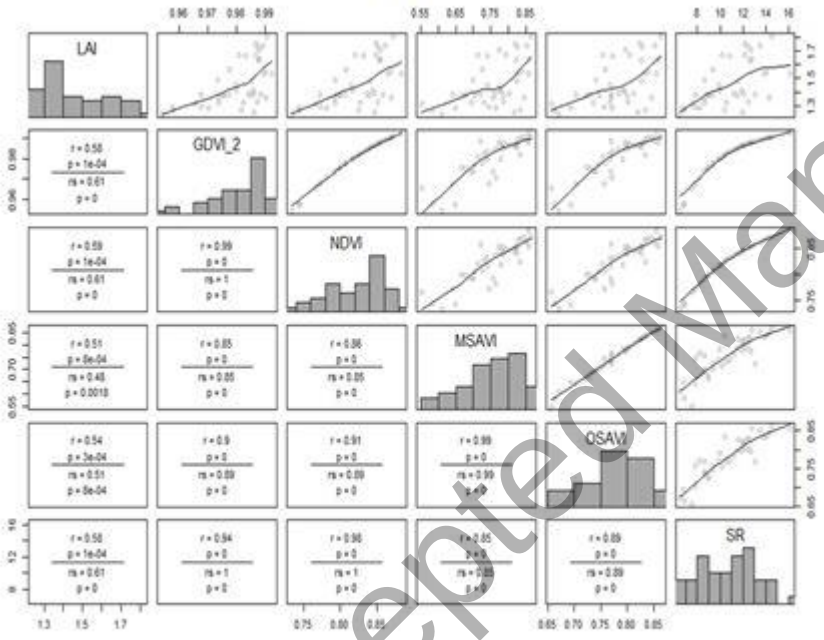

[b]

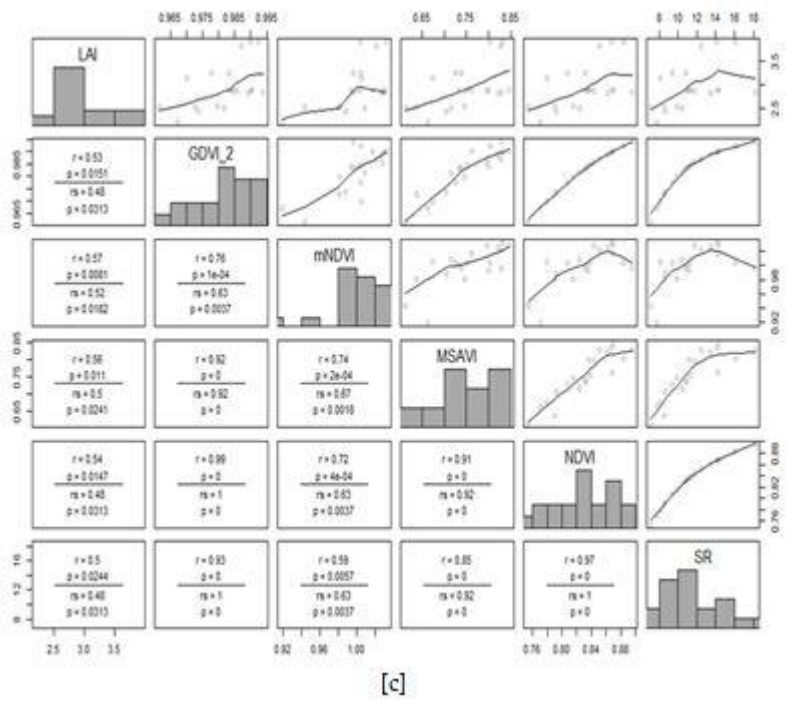

Figure 6. (a-c) Correlation matrix plot of best 5 LAI based indices at different stages of wheat crop (a) tillering stage (b) booting stage (c) heading stage

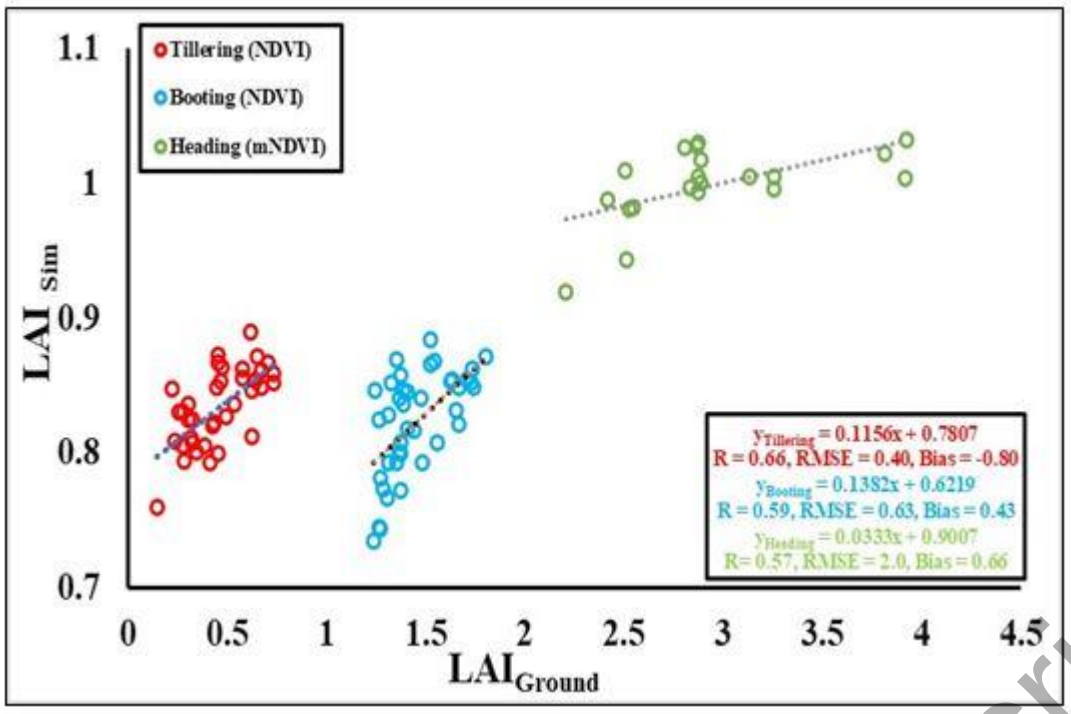

Figure 7: Best LAI model for different stages of wheat crop

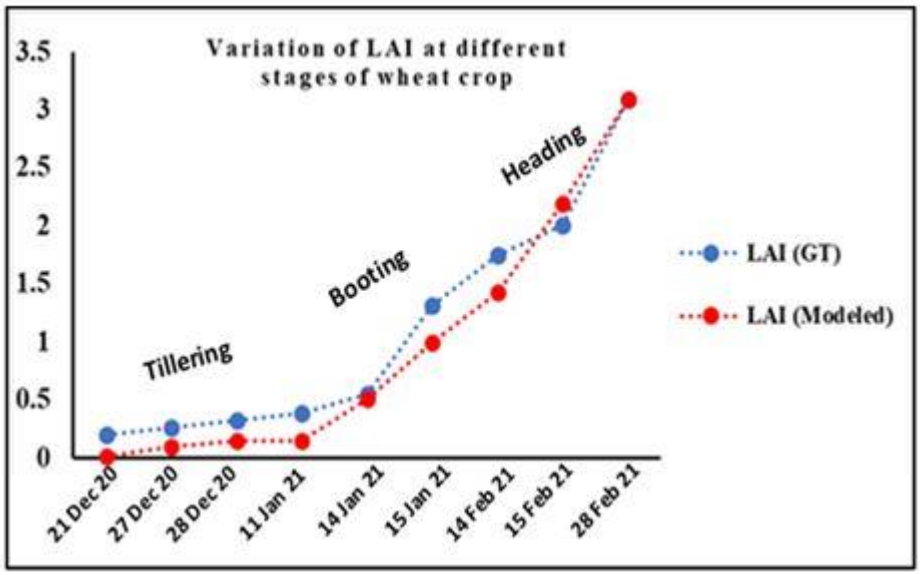

Figure 8: Variations of LAI at different stages of wheat crop

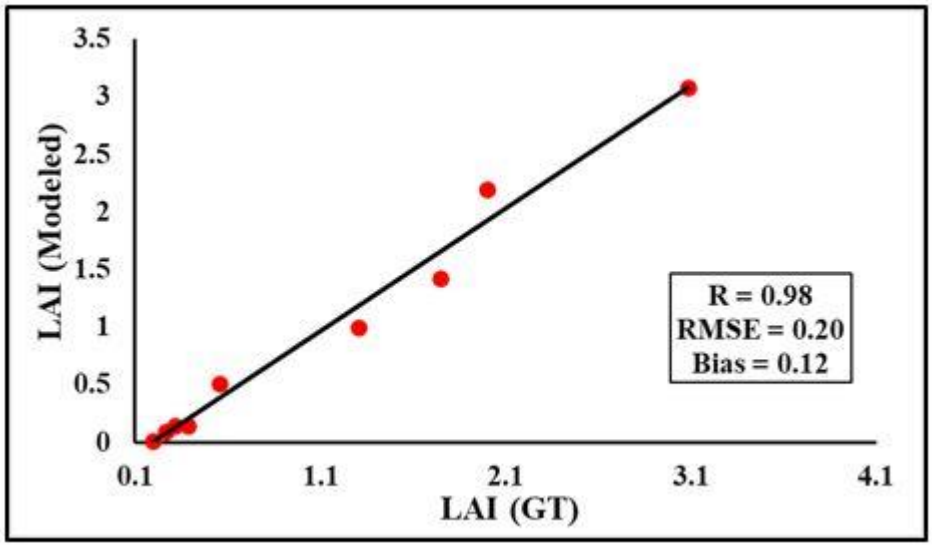

Figure 9: Performance of LAI for whole period

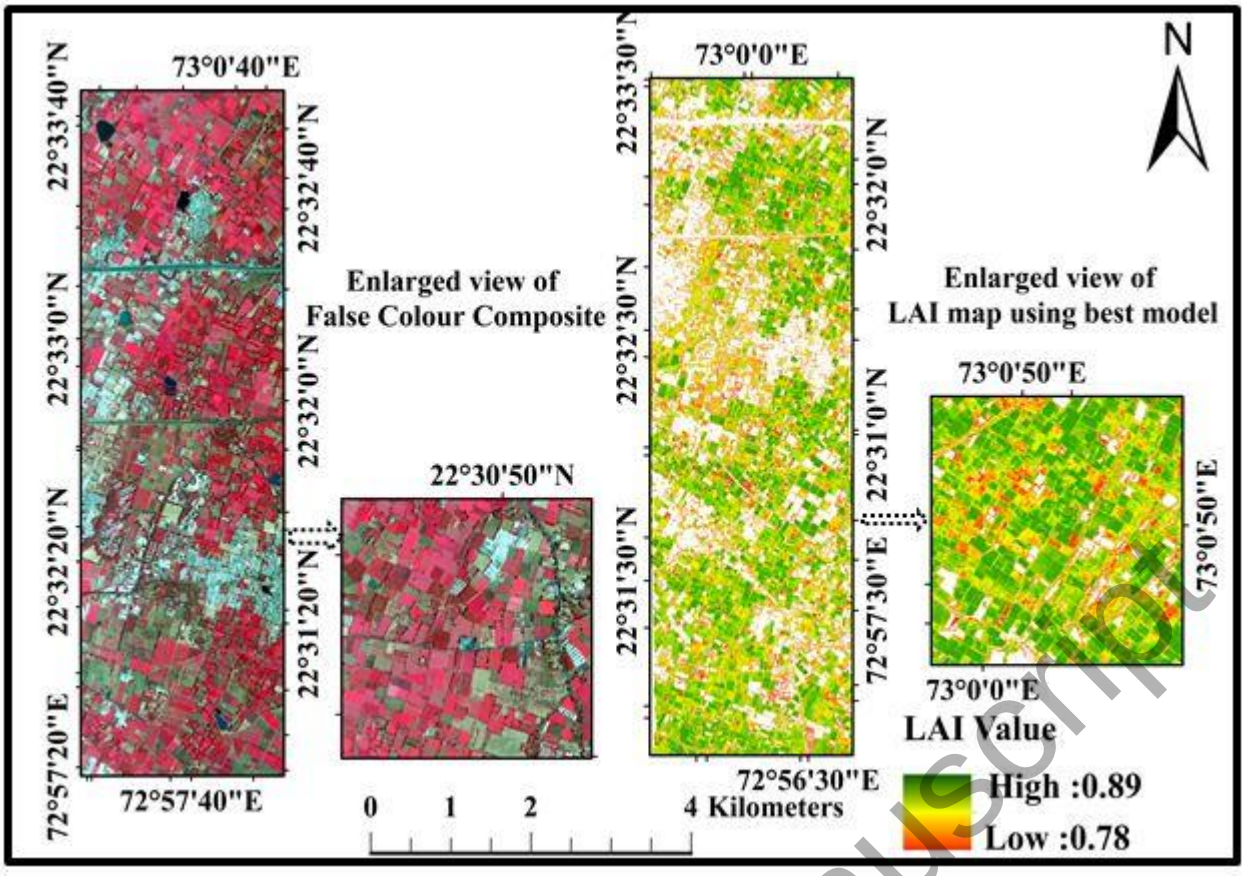

Figure 10: AVIRIS-NG RGB composite and LAI map using LAI best model

Table 1. Specification of AVIRIS-NG (Singh, Srivastava, et al. 2020b**;** Ahmad et al. 2021**)**

Parameters	**Specifications**
Wavelength Range	380 nm to 2510 nm
Spectral Resolution (FWHM, minimum)	5 nm ± 0.5 nm
Field of View (FOV)	36°± 2°
Instantaneous Field of View (IFOV)	1.0 milliradian
Ground Sampling distance (GSD)	4 to 8 m
Radiometric Resolution	14 bits
Maximum Altitude	18 km
Acquisition date	7th January 2016